Electronic Supplementary Material (ESI) for Soft Matter.
This journal is © The Royal Society of Chemistry 2018

Electronic Supplementary Information (ESI):

Wrinkling Patterns in Soft Shells

Cheng Zhang,[1,2] Yu-Kun Hao,[2] Bo Li,[1,*] Xi-Qiao Feng,[1,3,*] Huajian Gao[4]

[1] Institute of Biomechanics and Medical Engineering, AML, Department of Engineering Mechanics, Tsinghua University, Beijing 100084, China
[2] Center for Nano and Micro Mechanics, Tsinghua University, Beijing, 100084, China
[3] State Key Laboratory of Tribology, Tsinghua University, Beijing 100084, China[4] School of Engineering, Brown University, Providence, Rhode Island 02912, USA

1. Experimental methods

The hemispherical soft shells used in this study were prepared following the method proposed by Lee et al..[1] A Vinylpolysiloxane (VPS, Elite Double 8, 22, Zhermack) liquid polymer solution was mixed at room temperature (20℃) with a base/cure ratio 1:1 in weight and poured onto a rigid spherical mold made by 3D printing. After 20 minutes of curing time, the silicone-based polymer solution is solidified into a thin hemispherical shell with nearly uniform thickness, as shown in Fig. S1. The soft shell was then peeled off from the mold and clamped between two annular plates, as shown in Fig. S2. The annular plates were supported by four legs, which were attached to a micrometer with the aid of another plate. An outward point force was applied at the shell pole by twisting the rod of the micrometer, to which a small steel ball was attached at the top. During loading, images were captured using a digital camera (Nikon D750).

After the buckling experiment, we cut the hemispherical shell into ribbons with a blade and measured its thickness h with a microscope (Leica DM2700M). The thickness h can be adjusted by regulating the polymer viscosity and curing time. The shells in Figs. 1 and 2 in the main text had a thickness of 0.35 ± 0.04 mm. The moduli of VPS (Elite Double 8, 22) were measured by indentation (Bose ElectroForces 3100).

* Corresponding authors.
E-mail addresses: libome@tsinghua.edu.cn (B. Li) and fengxq@tsinghua.edu.cn (X. Q. Feng).

Fig. S1. Fabrication method of a hemispherical soft shell.[1]

Fig. S2. Clamped boundary at the brim of the hemispherical shell.

2. Basic equations

We use the nonlinear theory of shallow shells to analyze the mechanical response of the hemispherical shell near the critical condition for buckling. According to this theory, the strains at the middle surface of the shell in the spherical coordinate system (R,θ,φ) can be expressed as[2]

$$\varepsilon_{\theta\theta}=\frac{1}{R}\frac{\partial u_\theta}{\partial\theta}-\frac{W}{R}+\frac{1}{2}\left(\frac{1}{R}\frac{\partial W}{\partial\theta}\right)^2,$$
$$\varepsilon_{\varphi\varphi}=\frac{1}{R\sin\theta}\frac{\partial u_\varphi}{\partial\varphi}+\frac{\cot\theta}{R}u_\theta-\frac{W}{R}+\frac{1}{2}\left(\frac{1}{R\sin\theta}\frac{\partial W}{\partial\varphi}\right)^2, \quad \backslash*$$
$$\varepsilon_{\theta\varphi}=\frac{1}{R}\frac{\partial u_\varphi}{\partial\theta}-\frac{\cot\theta}{R}u_\varphi+\frac{1}{R\sin\theta}\frac{\partial u_\theta}{\partial\varphi}+\frac{1}{R^2\sin\theta}\frac{\partial W}{\partial\theta}\frac{\partial W}{\partial\varphi},$$

MERGEFORMAT (S1)

where R is the shell radius, $\varepsilon_{\alpha\beta}$ $(\alpha,\beta=\theta,\varphi)$the strains, u_α the displacements, and W the deflection in the normal direction. The stresses $\sigma_{\alpha\beta}$ are related to the strains $\varepsilon_{\alpha\beta}$ by

$$\sigma_{\theta\theta}=\frac{E}{1-\nu^2}\left(\varepsilon_{\theta\theta}+\nu\varepsilon_{\varphi\varphi}\right),$$
$$\sigma_{\varphi\varphi}=\frac{E}{1-\nu^2}\left(\varepsilon_{\varphi\varphi}+\nu\varepsilon_{\theta\theta}\right), \quad \backslash^* \text{ MERGEFORMAT (S2)}$$
$$\sigma_{\theta\varphi}=\frac{E}{2(1+\nu)}\varepsilon_{\theta\varphi},$$

where E and ν denote the Young's modulus and Poisson's ratio of the shell, respectively. The membrane forces $N_{\alpha\beta}$ can be obtained from $N_{\alpha\beta}=h\sigma_{\alpha\beta}$. The curvatures $\kappa_{\alpha\beta}$ at the middle surface are[2]

$$\kappa_{\theta\theta}=\frac{1}{R^2}\frac{\partial^2 W}{\partial\theta^2},$$
$$\kappa_{\varphi\varphi}=\frac{1}{R^2\sin^2\theta}\frac{\partial^2 W}{\partial\varphi^2}+\frac{\cot\theta}{R^2}\frac{\partial W}{\partial\theta}, \quad \backslash^*$$
$$\kappa_{\theta\varphi}=\frac{1}{2R^2}\left[\sin\theta\frac{\partial}{\partial\theta}\left(\frac{1}{\sin^2\theta}\frac{\partial W}{\partial\varphi}\right)+\frac{1}{\sin\theta}\frac{\partial^2 W}{\partial\varphi\partial\theta}\right].$$

MERGEFORMAT (S3)

The bending and twisting moments $M_{\alpha\beta}$ are then derived as

$$M_{\theta\theta}=\frac{Eh^3}{12(1-\nu^2)}\left(\kappa_{\theta\theta}+\nu\kappa_{\varphi\varphi}\right),$$
$$M_{\varphi\varphi}=\frac{Eh^3}{12(1-\nu^2)}\left(\kappa_{\varphi\varphi}+\nu\kappa_{\theta\theta}\right), \quad \backslash^* \text{ MERGEFORMAT (S4)}$$
$$M_{\theta\varphi}=\frac{Eh^3}{12(1-\nu^2)}\kappa_{\theta\varphi}.$$

The stretching and bending energy densities in the shell can be written as[3]

$$U_{\mathrm{s}}=\frac{Eh}{2(1-\nu^2)}\left[\varepsilon_{\theta\theta}^2+\varepsilon_{\varphi\varphi}^2+2\nu\varepsilon_{\theta\theta}\varepsilon_{\varphi\varphi}+\frac{1}{2}(1-\nu)\varepsilon_{\theta\varphi}^2\right],\backslash^*$$

MERGEFORMAT (S5)

$$U_{\mathrm{b}}=\frac{D}{2}\left[\kappa_{\theta\theta}^2+\kappa_{\varphi\varphi}^2+2\nu\kappa_{\theta\theta}\kappa_{\varphi\varphi}+2(1-\nu)\kappa_{\theta\varphi}^2\right],\backslash^*$$

MERGEFORMAT (S6)

respectively, where $D=Eh^3/[12(1-\nu^2)]$ is the bending stiffness. The elastic strain energy in the shell reads

$$U=\iint_{\Omega}\left(U_{\mathrm{s}}+U_{\mathrm{b}}\right)R^2\sin\theta\,\mathrm{d}\theta\,\mathrm{d}\varphi\,, \backslash^* \text{ MERGEFORMAT (S7)}$$

where Ω represents the surface occupied by the hemispherical shell. Minimizing Eq. * MERGEFORMAT (S7), we obtain the governing equations of the shell

$$\begin{aligned} &D\nabla^2\nabla^2 W+\frac{1}{R}\nabla^2\Psi-\{W,\Psi\}=0,\\ &\frac{1}{Eh}\nabla^2\nabla^2\Psi-\frac{1}{R}\nabla^2 W+\{W,W\}=0, \end{aligned} \quad \text{* MERGEFORMAT}$$

(S8)

where Ψ is the stress function, from which the membrane forces can be calculated as

$$\begin{aligned} N_{\theta\theta}&=\frac{1}{R^2\sin^2\theta}\frac{\partial^2\Psi}{\partial\varphi^2}+\frac{\cot\theta}{R^2}\frac{\partial\Psi}{\partial\theta},\\ N_{\varphi\varphi}&=\frac{1}{R^2}\frac{\partial^2\Psi}{\partial\theta^2},\\ N_{\theta\varphi}&=-\frac{1}{2R^2}\left[\sin\theta\frac{\partial}{\partial\theta}\left(\frac{1}{\sin^2\theta}\frac{\partial\Psi}{\partial\varphi}\right)+\frac{1}{\sin\theta}\frac{\partial^2\Psi}{\partial\varphi\partial\theta}\right]. \end{aligned}$$

In Eq. * MERGEFORMAT (S8), the Laplace operator ∇^2 is defined as

$$\nabla^2=\frac{1}{R^2}\frac{\partial^2}{\partial\theta^2}+\frac{\cot\theta}{R^2}\frac{\partial}{\partial\theta}+\frac{1}{R^2\sin^2\theta}\frac{\partial^2}{\partial\varphi^2}, \text{* MERGEFORMAT}$$

(S9)

and $\{\cdot\}$ is a bilinear operator and written in the spherical coordinate system as

$$\begin{aligned} \{f,g\}=&\frac{1}{R^2}\frac{\partial^2 f}{\partial\theta^2}\left(\frac{\cot\theta}{R^2}\frac{\partial g}{\partial\theta}+\frac{1}{R^2\sin^2\theta}\frac{\partial^2 g}{\partial\varphi^2}\right)+\frac{1}{R^2}\frac{\partial^2 g}{\partial\theta^2}\left(\frac{\cot\theta}{R^2}\frac{\partial f}{\partial\theta}\right.\\ &\left.+\frac{1}{R^2\sin^2\theta}\frac{\partial^2 f}{\partial\varphi^2}\right)-\frac{2}{R^4\sin^2\theta}\left(\frac{\partial^2 g}{\partial\theta\partial\varphi}-\cot\theta\frac{\partial g}{\partial\varphi}\right)\left(\frac{\partial^2 f}{\partial\theta\partial\varphi}-\cot\theta\frac{\partial f}{\partial\varphi}\right). \end{aligned} \quad \text{* MERGEFORMAT (S10)}$$

We next prescribe the boundary conditions for the hemispherical shell. At the equator $\theta=\pi/2$, one has

$$\begin{aligned} &W=0,\\ &\varepsilon_{\varphi\varphi}=0\Rightarrow\frac{\partial^2\Psi}{\partial\theta^2}-\nu\left(\frac{\cot\theta}{R^2}\frac{\partial\Psi}{\partial\theta}+\frac{1}{R^2\sin^2\theta}\frac{\partial^2\Psi}{\partial\varphi^2}\right)=0,\\ &N_{\theta\varphi}=0\Rightarrow-\frac{1}{R^2\sin\theta}\left(\frac{\partial^2\Psi}{\partial\theta\partial\varphi}-\cot\theta\frac{\partial\Psi}{\partial\varphi}\right)=0,\\ &M_{\theta\varphi}=0\Rightarrow\frac{\partial^2 W}{\partial\theta^2}+\nu\left(\frac{\cot\theta}{R^2}\frac{\partial W}{\partial\theta}+\frac{1}{R^2\sin^2\theta}\frac{\partial^2 W}{\partial\varphi^2}\right)=0. \end{aligned} \quad \text{* MERGEFORMAT (S11)}$$

At the apex $\theta = 0$, we set

$$
\begin{aligned}
&W = \Delta, \\
&\varepsilon_{\varphi\varphi} = 0 \Rightarrow \frac{\partial^2 \Psi}{\partial \theta^2} - \nu \left(\frac{\cot\theta}{R^2} \frac{\partial \Psi}{\partial \theta} + \frac{1}{R^2 \sin^2\theta} \frac{\partial^2 \Psi}{\partial \varphi^2} \right) = 0, \\
&N_{\theta\varphi} = 0 \Rightarrow -\frac{1}{R^2 \sin\theta} \left(\frac{\partial^2 \Psi}{\partial \theta \partial \varphi} - \cot\theta \frac{\partial \Psi}{\partial \varphi} \right) = 0, \\
&M_{\theta\varphi} = 0 \Rightarrow \frac{\partial^2 W}{\partial \theta^2} + \nu \left(\frac{\cot\theta}{R^2} \frac{\partial W}{\partial \theta} + \frac{1}{R^2 \sin^2\theta} \frac{\partial^2 W}{\partial \varphi^2} \right) = 0.
\end{aligned}
\qquad \backslash^* \text{ MERGEFORMAT (S12)}
$$

where Δ is the externally applied displacement at the apex. Before the membrane buckles, Eq. * MERGEFORMAT (S8), together with boundary conditions * MERGEFORMAT (S11) and * MERGEFORMAT (S12), has an axisymmetric solution. Numerically solving this differential system with the centered finite difference method, we can obtain the displacements, strains, and stresses in the membrane. We find that the longitudinal stress $\sigma_{\theta\theta}$ is tensile everywhere, and the latitudinal stress $\sigma_{\varphi\varphi}$ is compressive except in a small circular region around the loading apex, as shown in Fig. 4(a) in the main text.

3. Stability analysis

When the externally applied displacement exceeds a threshold, Δ_c, the axial-symmetry of deformation will be broken. To investigate the stability of the hemispherical shell subject to an outward concentrated force, we introduce small sinusoidal-mode perturbations to the differential system * MERGEFORMAT (S8), * MERGEFORMAT (S11), and * MERGEFORMAT (S12):

$$
\begin{aligned}
W &= W^{(0)}(\theta) + w(\theta)\cos(m\varphi), \\
\Psi &= \Psi^{(0)}(\theta) + \psi(\theta)\cos(m\varphi),
\end{aligned}
\qquad \backslash^* \text{ MERGEFORMAT (S13)}
$$

where $W^{(0)}$ and $\Psi^{(0)}$ are the axisymmetric solution of Eq. * MERGEFORMAT (S8), $\psi(\theta)\cos(\varphi)$ and $w(\theta)\cos(\varphi)$ are perturbations. Substituting Eq. * MERGEFORMAT (S13) into Eqs. * MERGEFORMAT (S8), * MERGEFORMAT (S11), and * MERGEFORMAT (S12), we obtain the perturbed governing equations

$$-D\tilde{\nabla}\tilde{\nabla}w-\frac{1}{R}\tilde{\nabla}\psi+\{W^{(0)},\psi\}+\{w,\Psi^{(0)}\}=0,$$
$$\frac{1}{Eh}\tilde{\nabla}\tilde{\nabla}\psi-\frac{1}{R}\tilde{\nabla}w+\{W^{(0)},w\}=0,$$

* MERGEFORMAT (S14)

with the perturbed boundary conditions

$$w=0,$$
$$\frac{\partial^2 w}{\partial\theta^2}+\nu\left(\frac{\cot\theta}{R^2}\frac{\partial w}{\partial\theta}-\frac{m^2}{R^2\sin^2\theta}w\right)=0,$$
$$\frac{\partial^2\psi}{\partial\theta^2}-\nu\left(\frac{\cot\theta}{R^2}\frac{\partial\psi}{\partial\theta}-\frac{m^2}{R^2\sin^2\theta}\psi\right)=0,$$
$$-\frac{\partial\psi}{\partial\theta}+m\psi\cot\theta=0$$

* MERGEFORMAT (S15)

at $\theta=\pi/2$ and $\theta=0$.

The perturbed operator $\tilde{\nabla}$ in Eq. * MERGEFORMAT (S14) refers to

$$\tilde{\nabla}=\frac{1}{R^2}\frac{\partial^2}{\partial\theta^2}+\frac{\cot\theta}{R^2}\frac{\partial}{\partial\theta}-\frac{m^2}{R^2\sin^2\theta}.$$ * MERGEFORMAT (S16)

In the stability analysis, we first obtain the axisymmetric solution $W^{(0)}$ and $\Psi^{(0)}$, and then examine the existence of perturbation function w and ψ. We combine the centered finite difference method and determinant method to solve the quadratic eigenvalue problem Eqs. * MERGEFORMAT (S14) and * MERGEFORMAT (S15). We restrict the wrinkle number m to be an integer and use the bisection method to determine Δ under which there exists a wrinkle mode m at which the determinant of the system vanishes. The critical mode m_c is determined by seeking the minimal value Δ_c that allows the perturbation solution to exist.

In addition, the system has only two non-dimensional parameters, i.e., h/R and ν. Thus the normalized critical displacement can be determined by

$$\frac{\Delta_c}{R}=\phi\left(\frac{h}{R},\nu\right),$$ * MERGEFORMAT (S17)

where ϕ is a non-dimensional function. In the thin membrane limit, i.e. $h/R \to 0$, it can be shown that buckling occurs at the very beginning of the loading process,[4] that is, $\phi \to 0$ as $h/R \to 0$. Since the VPS material used in our experiments is nearly incompressible, we take its Poisson's ratio as $\nu = 0.5$. Therefore, under the thin membrane approximation, Eq. * MERGEFORMAT (S17) can be expanded as $\frac{\Delta_c}{R} = f(\nu)\frac{h}{R} + o\left(\frac{h}{R}\right)$ when $h/R \to 0$. Thus, we obtain the scaling law

$$\frac{\Delta_c}{R} \sim \frac{h}{R}, \qquad \text{* MERGEFORMAT (S18)}$$

which is similar to the scaling law for a spherical shell under an inward point force.[4]

Our finite element simulations validated these results. As shown in Fig. 4(b) in the main text, the numerical results agree well with the theoretical prediction, including the scaling law in Eq. * MERGEFORMAT (S18). In addition, we also perform FEM simulations on the neo-Hookean hemispherical shell subject to the displacement Δ at the apex, obtaining almost the same results as those for the linear shell, as shown in Fig. 4(b). We note that such non-axisymmetric shallow wrinkles have been observed by Bushnell.[5]

4. Deformation at the pseudocone stage

4.1. Tension-field theory

According to the latitudinal stress distribution, the buckled shell can be divided into three zones: (I) the transition zone near the clamped boundary, (II) a wrinkly zone in the middle, and (iii) the top zone near the apex. We first focus on the wrinkly zone. Following Libai's work,[6] we can obtain the basic geometric features of the shell at the limit of zero bending rigidity when the hemispherical membrane is largely deformed. Under this assumption, we adopt the tension-field theory to delineate the wrinkly zone. The wrinkly pseudosurface constitutes a portion of a cone.

On the pseudosurface, one has the following geometrical relations

$$\varepsilon_{\varphi\varphi} = \frac{\overline{r}}{r} - 1, \ \varepsilon_{\theta\theta} = \frac{\mathrm{d}\overline{S}}{\mathrm{d}S} - 1, \quad \text{* MERGEFORMAT (S19)}$$

where S denotes the arc length in the longitudinal direction and r is the radius of a latitudinal hoop in the reference configuration. The overbar pertains to the corresponding quantities in the deformed configuration.

Denote the outward force applied at the apex of the hemispherical membrane by F. Let α represent the direction of S measured from the horizontal direction, as shown in Fig. S3. The force equilibrium in the vertical direction requires

$$F = 2\pi \bar{r} \bar{N}_{\theta\theta} \sin\bar{\alpha} . \qquad \text{* MERGEFORMAT (S20)}$$

The corresponding transformation equation reads

$$\bar{r} \bar{N}_{\theta\theta} = r N_{\theta\theta} . \qquad \text{* MERGEFORMAT (S21)}$$

Thus, Eq. * MERGEFORMAT (S21) becomes

$$F = 2\pi r N_{\theta\theta} \sin\bar{\alpha} . \qquad \text{* MERGEFORMAT (S22)}$$

In the tension-field region (the wrinkly zone), the compressive membrane force in the hoop direction is ignored. Hence,

$$N_{\varphi\varphi} = 0 . \qquad \text{* MERGEFORMAT (S23)}$$

Using $N_{\theta\theta} = Eh\varepsilon_{\theta\theta}$, Eq. * MERGEFORMAT (S22) leads to

$$\frac{F}{2\pi r \sin\bar{\alpha}} = Eh\left(\frac{\mathrm{d}\bar{S}}{\mathrm{d}S} - 1\right) = -\frac{Eh}{\nu}\left(\frac{\bar{r}}{r} - 1\right). \qquad \text{* MERGEFORMAT (S24)}$$

Following Libai,[6] we introduce a non-dimensional parameter $\varepsilon = \dfrac{F}{2\pi ERh}$ to represent the prevailing strain in the regions below the top zone. From Eq. * MERGEFORMAT (S24) and $\sin\alpha = r / R$, we obtain

$$\nu\varepsilon \frac{1}{\sin\bar{\alpha}} = \sin\alpha - \frac{\bar{r}}{R} . \qquad \text{* MERGEFORMAT (S25)}$$

We introduce α_0 and $\bar{\alpha}_0$ to denote the local direction of S and $\bar{S}$ at the bottom of the wrinkly zone, respectively. Let $\bar{r}_0$ represent the radius at the bottom of the wrinkly zone, as shown in Fig. S3. Simple geometrical analysis yields

$$\cos\bar{\alpha}_0 \approx \frac{\bar{r}_0}{\alpha_0 R + \Delta L}, \qquad \text{* MERGEFORMAT (S26)}$$

where ΔL represents the total elongation of the longitudinal generator. Substituting α_0 and $\bar{\alpha}_0$ into Eq. * MERGEFORMAT (S25), we obtain

$$\nu\varepsilon \frac{1}{\sin\bar{\alpha}_0} = \sin\alpha_0 - \frac{\bar{r}_0}{R}. \qquad \text{* MERGEFORMAT (S27)}$$

Combining Eqs. * MERGEFORMAT (S26) and * MERGEFORMAT (S27), we have

$$\cos\bar{\alpha}_0 = \frac{\sin\alpha_0 - \dfrac{\nu\varepsilon}{\sin\bar{\alpha}_0}}{\alpha_0 + \dfrac{\Delta L}{R}}. \qquad \text{* MERGEFORMAT (S28)}$$

According to Libai,[6] the term $\Delta L / R$ has the order of $O(\varepsilon)$, while the angle α_0 is $\pi/2 - O(\varepsilon)$, because the vertical height of the transition zone is of the order $O(\varepsilon)R$. Thus

$$\cos\bar{\alpha}_0 = \frac{2}{\pi} + O(\varepsilon). \qquad \text{* MERGEFORMAT (S29)}$$

In terms of our numerical simulations and experiments, ε can be estimated as

$$\varepsilon = \frac{F}{2\pi ERh} \sim \frac{10^{-1}}{10^{6}\times 10^{-2}\times 10^{-3}} = 10^{-2}. \text{* MERGEFORMAT (S30)}$$

Therefore, we can obtain the slope angle at the bottom of the wrinkly zone

$$\bar{\alpha}_0 = \arccos\frac{2}{\pi} + O(\varepsilon) = 50.5^\circ + O(\varepsilon). \text{* MERGEFORMAT (S31)}$$

In fact, this angle approximately describes the slope of the pseudocone, as shown in Fig. S3. However, when the force F is extremely large, ε is never a small quantity and $\bar{\alpha}_0$ approaches $\pi/2$. In this extreme situation, the wrinkly zone will disappear.

From Eq. * MERGEFORMAT (S25), we obtain

$$\bar{r} = r - \nu \frac{\varepsilon R}{\sin \bar{\alpha}_0}. \qquad \text{* MERGEFORMAT (S32)}$$

Equation * MERGEFORMAT (S32) describes the deformation of the hemispherical membrane at the pseudocone stage. It can be seen that $\bar{r} \geq 0$ must hold, which requires $r \geq \nu \frac{\varepsilon R}{\sin \bar{\alpha}_0}$. Hence, the vertical height of the top zone can be estimated as $\sim \nu \frac{\varepsilon R}{\sin \bar{\alpha}_0}$. It shows that the height of the top zone increases as the force increases, since the prevailing strain ε is proportional to the force F.

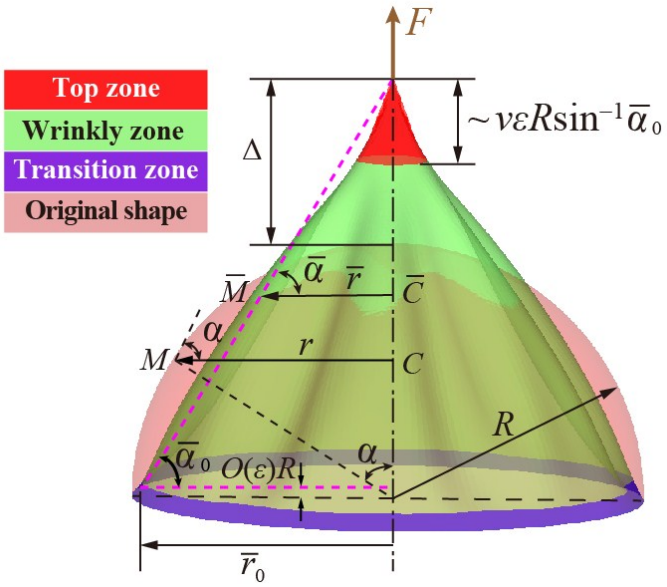

Fig. S3. The reference configuration and the deformed configuration. After deformation, the points C and M in the reference configuration are transformed to $\bar{C}$ and $\bar{M}$ in the deformed configuration, respectively.

4.2. Wrinkling analysis in the pseudocone state

Different from the tension-field analysis in Subsection 4.1, we need to take into account the bending stiffness to analyze the wrinkling characteristics. When the number of wrinkles reaches its maximum value, $n_{\max}$, the shell can be approximately modeled as a cone. To determine $n_{\max}$, we consider the energetic balance between bending and stretching caused by the tensile force along the longitudinal generator. To the lowest order, the latitudinal curvature is dominant in the deformed

configuration and, thus, the bending energy density scales as

$$u_{\mathrm{b}} \sim D\left(\frac{A}{\lambda^2}\right)^2 \sim D\left(\frac{An_{\max}^2}{R^2}\right)^2, \quad \text{* MERGEFORMAT (S33)}$$

where A and λ denote the amplitude and the wavelength of wrinkles, respectively, and $n_{\max} \sim 2\pi R/\lambda$. From Eqs. * MERGEFORMAT (S1) and * MERGEFORMAT (S5), the stretching energy density arising from the longitudinal deformation is characterized as

$$u_{\mathrm{s}} \sim Eh\left(\frac{A}{R}\right)^2. \quad \text{* MERGEFORMAT (S34)}$$

Balance between the bending and stretching energies gives

$$Eh\left(\frac{A}{R}\right)^2 \sim D\left(\frac{An_{\max}{}^2}{R^2}\right)^2, \quad \text{* MERGEFORMAT (S35)}$$

which further leads to

$$n_{\max} \sim \left(\frac{h}{R}\right)^{-\frac{1}{2}}, \quad \text{* MERGEFORMAT (S36)}$$

as shown in Fig. 5(d) in the main text. This theoretical prediction agrees well with our experiments and FEM simulations.

5. Four-stage morphological transition

Our numerical simulations demonstrate a four-stage morphological transition with increasing displacement load at the hemispherical shell's apex, as shown in Fig. S4. The shell starts with axisymmetric deformation around its pole (Stage I) and then evolves into a non-axisymmetric shape with a number of shallow wrinkles emanating from the pole (Stage II), followed by the consecutive emergence of crater-like deep crumples (Stage III) and ultimately a transformation into a wrinkled pseudocone (Stage IV). In addition, the four-stage morphological transitions under the linear Hookean and nonlinear neo-Hookean constitutive relations are very similar.

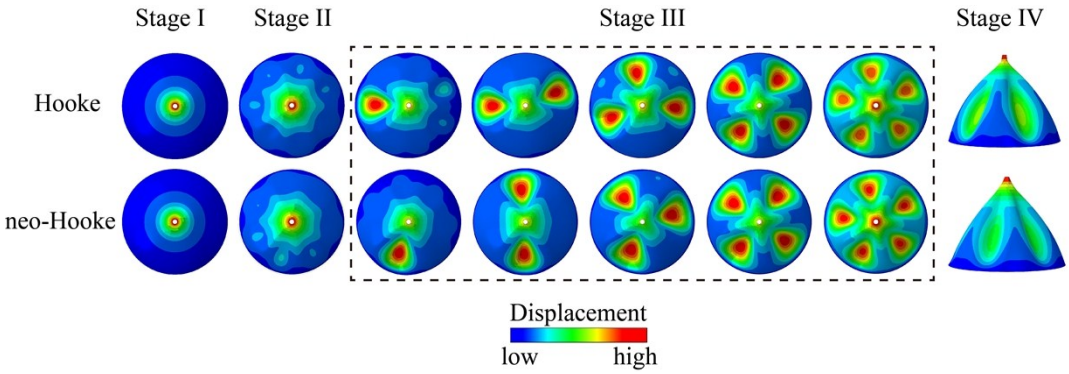

Fig. S4. FEM simulations of the four-stage morphological transition in the hemispherical shell subject to an outward displacement, the shell being modeled by linear Hookean and nonlinear neo-Hookean material laws. The color denotes the total displacement.

6. Dependence of *R* on *h* and *R* at Stage IV

To validate the choice of the ratio h/R, we examine the dependences of $n_{\max}$ on h and R separately. Our results show that their separate dependences are consistent with the scaling law $n_{\max} \sim (h/R)^{-1/2}$, as shown in Fig. S5.

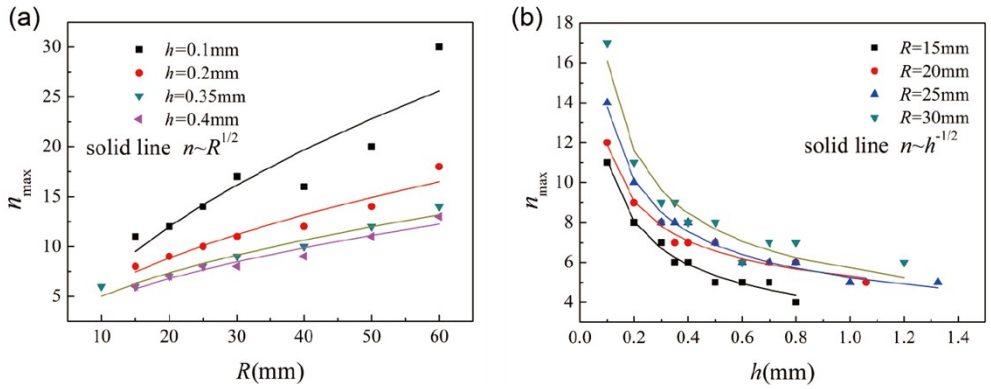

Fig. S5. Dependence of $n_{\max}$ on (a) the shell radius R and (b) thickness h.

7. Influence of boundary conditions

To examine the influence of boundary conditions, we perform FEM simulations to compare the buckling behaviors of a hemispherical shell under the clamped and hinged conditions. In both cases, the three displacement components along its brim

are fixed. The results are shown in Fig. S6. It can be seen that these two situations share the same characteristics of wrinkling pattern evolutions.

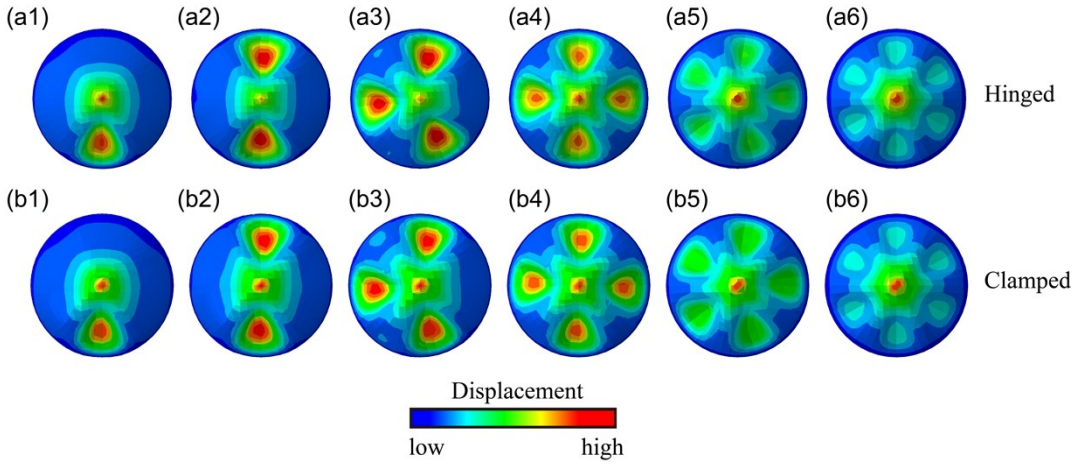

Fig. S6. Comparison between the morphological evolutions of a hemispherical shell under the (a1–a6) hinged and (b1–b6) clamped boundary conditions.

References

1. A. Lee, P.-T. Brun, J. Marthelot, G. Balestra, F. Gallaire, and P. M. Reis, *Nat. Commun*. 2016, **7**, 11155.
2. P. E. Tovstik and A. L. Smirnov, *Asymptotic Methods in the Buckling Theory of Elastic Shells*, World Scientific, 2001.
3. E. Ventsel and T. Krauthammer, *Thin Plates and Shells: Theory, Analysis, and Applications*, CRC Press, 2001.
4. D. Vella, A. Ajdari, A. Vaziri, and A. Boudaoud, *Phys. Rev. Lett*. 2011, **107**, 174301.
5. D. Bushnell, *AIAA J*. 1967, **5**, 2034–2040.
6. A. Libai, *Int. J. Solids Struct*. 1990, **26**, 927–939.